

# Evaluation of the Efficiency of Conductor Placement Under Different Types of Pulse Interference in Differential and Common Modes

Alexandr M. Lakoza  
*dept. of Microwave and Quantum Radio Engineering*  
*Tomsk State University of Control*  
*Systems and Radioelectronics*  
 Tomsk, Russian Federation  
 alexandrakoza@mail.ru

Valerii P. Kosteletskii  
*dept. of Microwave and Quantum Radio Engineering*  
*Tomsk State University of Control*  
*Systems and Radioelectronics*  
 Tomsk, Russian Federation  
 kosteletskiy.vp@gmail.com

**Abstract**—This paper investigates of the efficiency of using different ways of placing conductors with identical and unequal characteristics before and after switching under different types of pulse disturbances in differential and common modes of influence, obtained on the example of a four-wire modal filter (MF). The results show that the location of the main and redundant conductors in the MF and the type of the interfering signal significantly affect its efficiency. When a digitized interference signal C9-11 is used, an increase in the amplitude at the output of the structure is observed for two configurations in common (by 11.3% and 10.4%, respectively) and one in differential modes (by 18.7%). However, when a bipolar pulse is used, amplitude changes are observed for only one configuration, in differential mode (2.4% increase). Using the conductor configurations discussed above can help account for channel degradation due to aging or component wear, allowing prediction of performance degradation in different modes of operation. Switching to the appropriate configuration at the right time allows the performance changes to be compensated for.

**Keywords**—*modal redundancy, modal filter, protection device, common mode, differential mode, ultra-wideband*

## I. INTRODUCTION

Modern electronic systems and devices are crucial to the operating of many important processes. They are becoming increasingly complex and demanding in terms of operating conditions. Therefore, there is a growing need to develop and apply effective methods to improve their protection, efficiency, and reliability [1]. Higher quality of electrical energy is essential to ensure safe and reliable operation of electrical systems. Power outages or power surges can lead to accidents, damage to equipment and even human damage [2]. The operation of these systems can be impaired by various disturbances, including pulse excitation [3]. To reduce the pulse excitation and enhance device reliability while facilitating modal filtering (MF), developers commonly employ redundancy [4]. This is achieved by incorporating reserved circuits alongside active ones, known as single modal redundancy (MR) [5]. This approach is widely used in industries such as power supply, telecommunications, and industrial automation [6, 7]. However, inconsistent switching can cause changes in the characteristics of reserved and active circuits in certain configurations.

Additionally, natural degradation of electrical circuits can result in inconsistent electrical parameter sets. These factors can lead to unpredictable quality in MR implementation. It is therefore imperative to perform an initial assessment of the electrical circuits to ensure their stable operation when incorporating MR configurations with both unequal and equal characteristics before and after switching. For a more precise analysis, it is essential to consider not only the switching between active and passive circuits but also the circuits characteristics and potential changes in the devices operating conditions. This preliminary analysis will help to predict the potential minimum voltage levels. The objective of this study is to investigate how MR configurations affect the output signal amplitude under different types of pulse interference in differential and common modes.

## II. CHOICE AND VALIDATION

To evaluate the influence of the conductor placement of the protective device on the attenuation coefficients, at various types of pulse interference in differential and common modes, a cross section of the modal filter is developed, which allows to configure the conductors so that before and after switching the electrical parameters of the protective device can be with the same and unequal characteristics. Heuristic search algorithms [8] were applied to quickly find the cross section parameters. As a result, the cross section MF with the following parameters is obtained ( $w=5$  mm,  $w_1=10$  mm,  $t=35$   $\mu$ m,  $s=0.55$  mm,  $g=1$  mm,  $h=0.36$  mm,  $H=2.65$  mm,  $\epsilon_{r1}=4.6$  and  $\epsilon_{r2}=1$ ) due to a current load of 2.5 A, according to the IPC-2221A standard [9]. At the near end of the passive line, open circuit (OC) termination loads are selected, and at the far end, short circuit (SC) termination loads are selected [10]. This termination configuration provides the greatest attenuation of unwanted pulse excitations. FR-4 fiberglass textolite is used as dielectric substrate material [11] (Fig. 1).

Two signals were used as test excitation EMF. One of them is a digitized signal from a computing combined oscilloscope C9-11, having a pulse duration of 300 ps at a level of 0.5, with an EMF amplitude of  $E=0.5$  V (Fig. 2, a). The second is a typical ultra-wideband (UWB) bipolar electromagnetic pulse (EMP), regulated by the standard IEC 61000-2-13 [12], with a duration of 1 ns (Fig. 2, b).

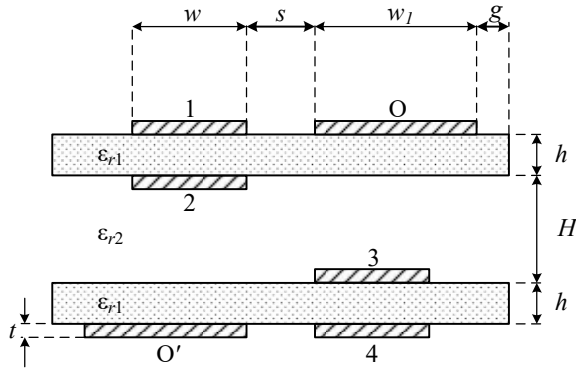


Fig. 1. Cross section of the structure MF operating in differential and common modes

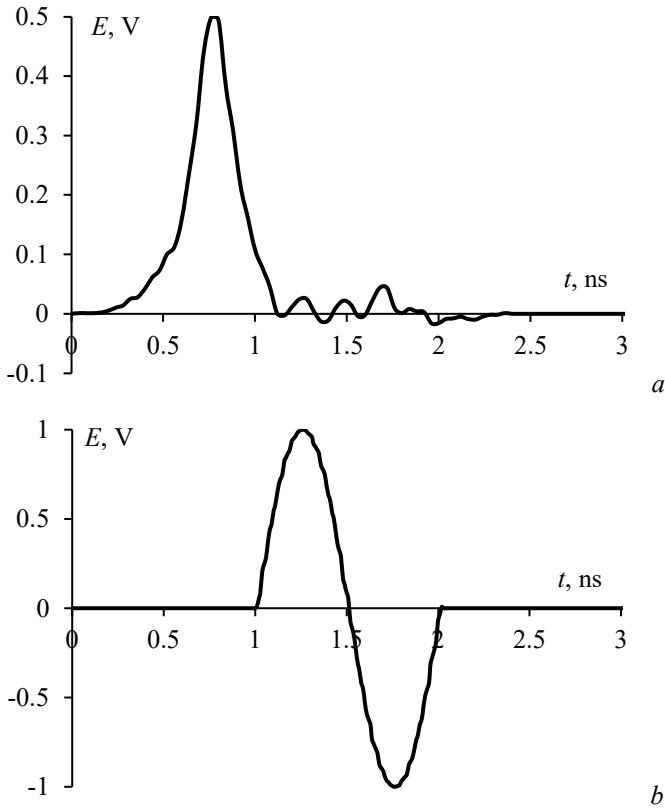


Fig. 2. EMF waveforms of the input signals: digitized signal C9-11 (a), bipolar (b) UWB EMP.

To modeling the common mode, EMF  $E_{G1}$  and  $E_{G2}$  were equal to each other and were fed to the input MF. For modeling the differential mode,  $E_{G1}$  and  $E_{G2}$  had different polarity [13]. However, it should be noted that the EMF of each excitation pulse in the differential mode is equal to half of the EMF in the common mode. It should be noted that the EMF of the excitation pulses in the differential mode is equal to half of the EMF in the common mode.

The common voltage at the MF output is defined as

$$V_{CM} = \frac{1}{2}(V_1 + V_2) \quad (1)$$

where  $V_2$  is the signal at the output of the second conductor relative to the reference,  $V_1$  is the signal at the output of the first conductor relative to the reference [14]

The differential mode voltage at the MF output is defined as

$$V_{DM} = V_1 - V_2 \quad (2)$$

The amplitude deviations are calculated as

$$\delta = \left| \frac{x_1 - x_2}{x_1 + x_2} \right| \cdot 100\% \quad (3)$$

where  $x_1$  is the maximum amplitude at the output of the structure before switching,  $x_2$  is the maximum amplitude at the output of the structure after switching [15].

For switching between the reserved and reserving conductor pairs at the near and far ends of the MF, switches are supposed to be used. Fig. 3 shows the electrical connection diagram of a redundant MF operating in differential and common modes. Two redundancy configurations, with equal and unequal characteristics, are investigated. The configuration with equal characteristics is obtained by switching the EMF sources from a pair of conductors 1 and 3 to a pair of conductors 2 and 4, while the distance between them remains unchanged. A configuration with unequal characteristics is obtained by switching the EMF sources from the most distant pair of conductors 1 and 4 to the closest pair of conductors 2 and 3, thereby reducing the distance between the lines. At the near end, the switch switches the EMF sources to different pairs of conductors, while the conductors not connected to the EMF sources remain in the OC mode. At the far end, the commutator switches different conductors between matched loads and SC mode. The near and far ends of the active conductors are connected resistors  $R=50 \Omega$ .

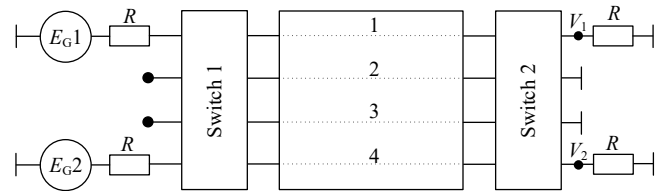


Fig. 3. Electrical connection diagram of MF with redundancy, operating in differential and common modes

Computer modelling was performed in the TALGAT system, without considering losses in conductors and dielectrics [16, 17]. Fig. 4 shows the voltage waveforms at the MF output for the configuration with switching from conductor pair 1 and 4 to pair 2 and 3, when exposed to the digitized signal C9-11. Fig. 5 shows the voltage waveforms at the MF output for the configuration with switching from conductor pair 1 and 3 to conductor pair 2 and 4, when the digitized signal C9-11 is applied.

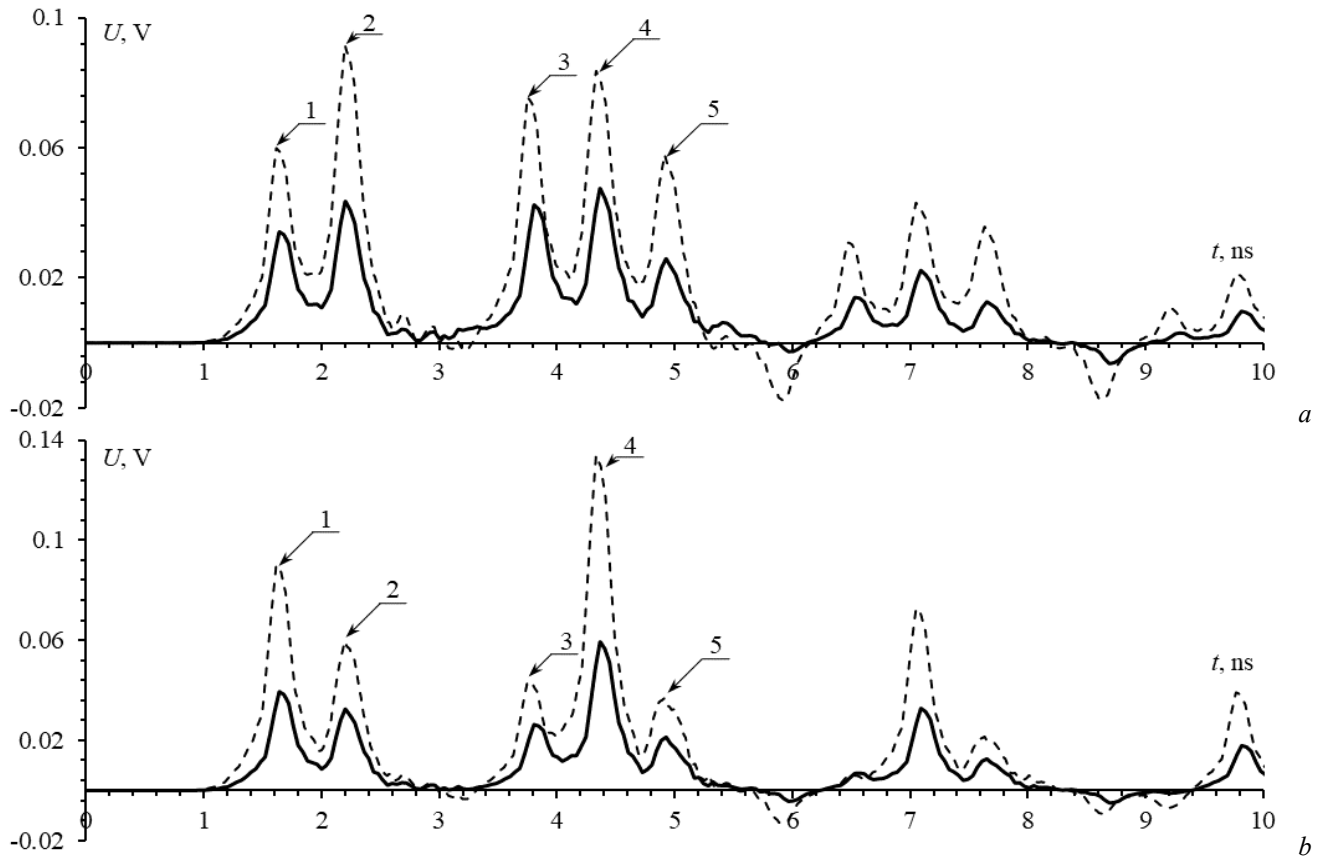


Fig. 4. Voltage waveforms at the MF output in common (—) and differential (---) modes, for conductors: 1 and 4 (a), 2 and 3 (b)

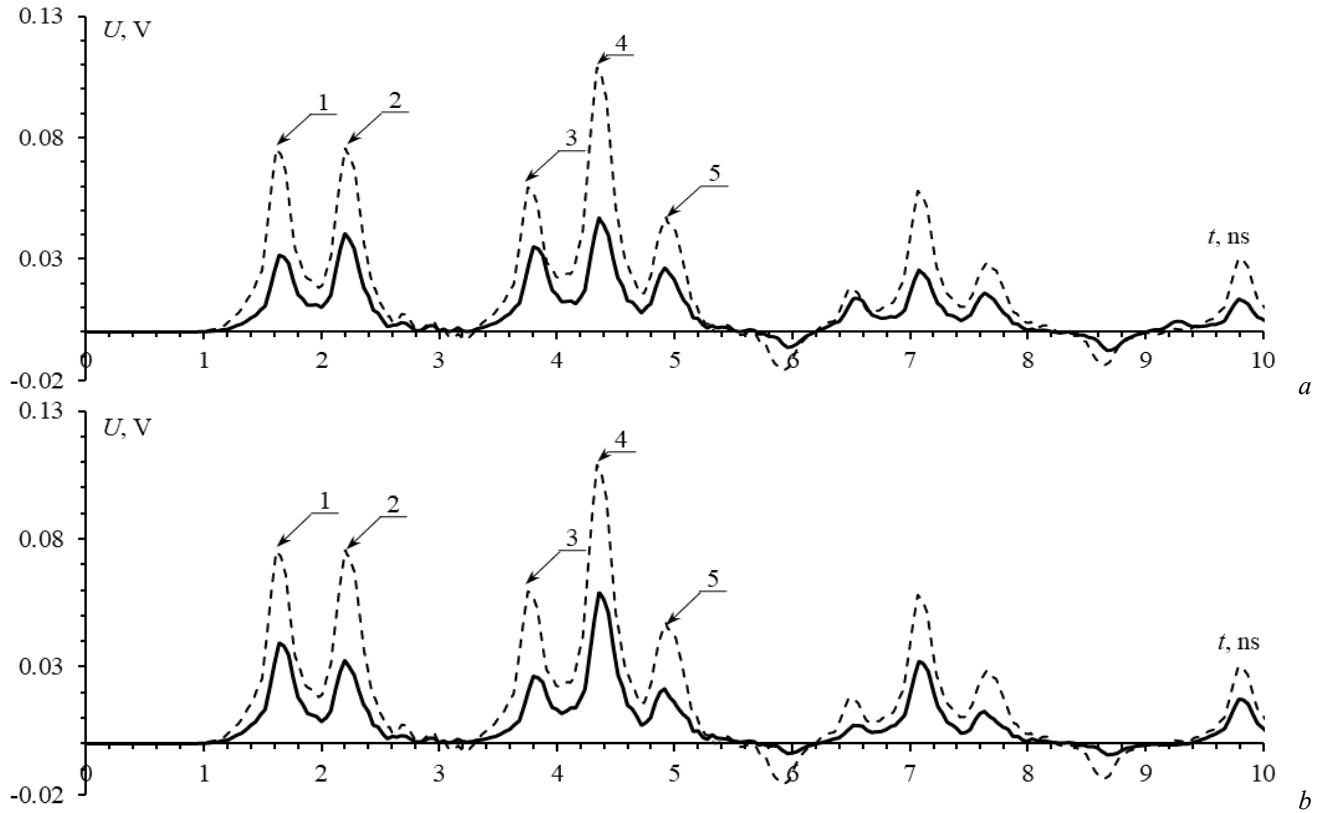


Fig. 5. Voltage waveforms at the MF output in common (—) and differential (---) modes, for conductors: 1 and 3 (a), 2 and 4 (b)

Tables I and II show the amplitudes of the first 5 pulses in common and differential modes.

TABLE I. AMPLITUDES IN COMMON MODE

Conductors	$U_1, \text{mV}$	$U_2, \text{mV}$	$U_3, \text{mV}$	$U_4, \text{mV}$	$U_5, \text{mV}$
1 and 4	33	43	41	47	24
2 and 3	39	31	26	59	21
1 and 3	31	40	35	47	26
2 and 4	39	31	26	58	21

Fig. 6 shows the voltage waveforms at the MF output for the configuration with switching from conductor pair 1 and 4 to pair 2 and 3, when subjected to a bipolar pulse.

TABLE II. AMPLITUDES IN DIFFERENTIAL MODE

Conductors	$U_1, \text{mV}$	$U_2, \text{mV}$	$U_3, \text{mV}$	$U_4, \text{mV}$	$U_5, \text{mV}$
1 and 4	59	91	74	82	55
2 and 3	87	58	43	133	36
1 and 3	74	75	59	108	47
2 and 4	74	75	59	108	47

Fig. 7 shows the voltage waveforms at the MF output for the configuration with switching from conductor pair 1 and 3 to pair 2 and 4, when subjected to a bipolar pulse.

Tables III and IV show the amplitudes of the first 5 pulses in common and differential modes.

TABLE III. AMPLITUDES IN COMMON MODE

Conductors	$U_1, \text{mV}$	$U_2, \text{mV}$	$U_3, \text{mV}$	$U_4, \text{mV}$	$U_5, \text{mV}$
1 and 4	62	30	-78	68	34
2 and 3	78	-31	-62	50	69
1 and 3	60	30	-78	65	34
2 and 4	75	-30	-61	50	68

TABLE IV. AMPLITUDES IN DIFFERENTIAL MODE

Conductors	$U_1, \text{mV}$	$U_2, \text{mV}$	$U_3, \text{mV}$	$U_4, \text{mV}$	$U_5, \text{mV}$
1 and 4	116	101	-182	148	79
2 and 3	173	-101	-117	91	191
1 and 3	148	75	-150	123	132
2 and 4	148	75	-150	123	132

It can be seen from the results that the location of redundant and backup conductors in the MF has a significant influence. The amplitude deviations are calculated obtained by (3). When using digitized interference signal C9-11 as input influence, an increase in the amplitude at the output of the structure is observed for configurations with unequal and equal characteristics. After common mode switching, by 11.3% (from conductor pair 1 and 4 to pair 2 and 3) and 10.4% (from conductor pair 1 and 3 to pair 2 and 4), respectively. For the case with unequal (from conductor pair 1 and 4 to pair 2 and 3) characteristics after switching in differential mode, by 18.7%. The configuration with equal characteristics after switching (from conductor pair 1 and 3 to pair 2 and 4) in differential mode shows no change in amplitude. When a bipolar pulse is used as an interfering signal, the opposite picture is observed: a change in the maximum amplitude at the output of the structure was observed only for the configuration with unequal (from conductor pair 1 and 4 to pair 2 and 3) characteristics before and after switching in differential mode - by 2.4%. The remaining configurations demonstrated no change in the maximum amplitude at the output of the structure.

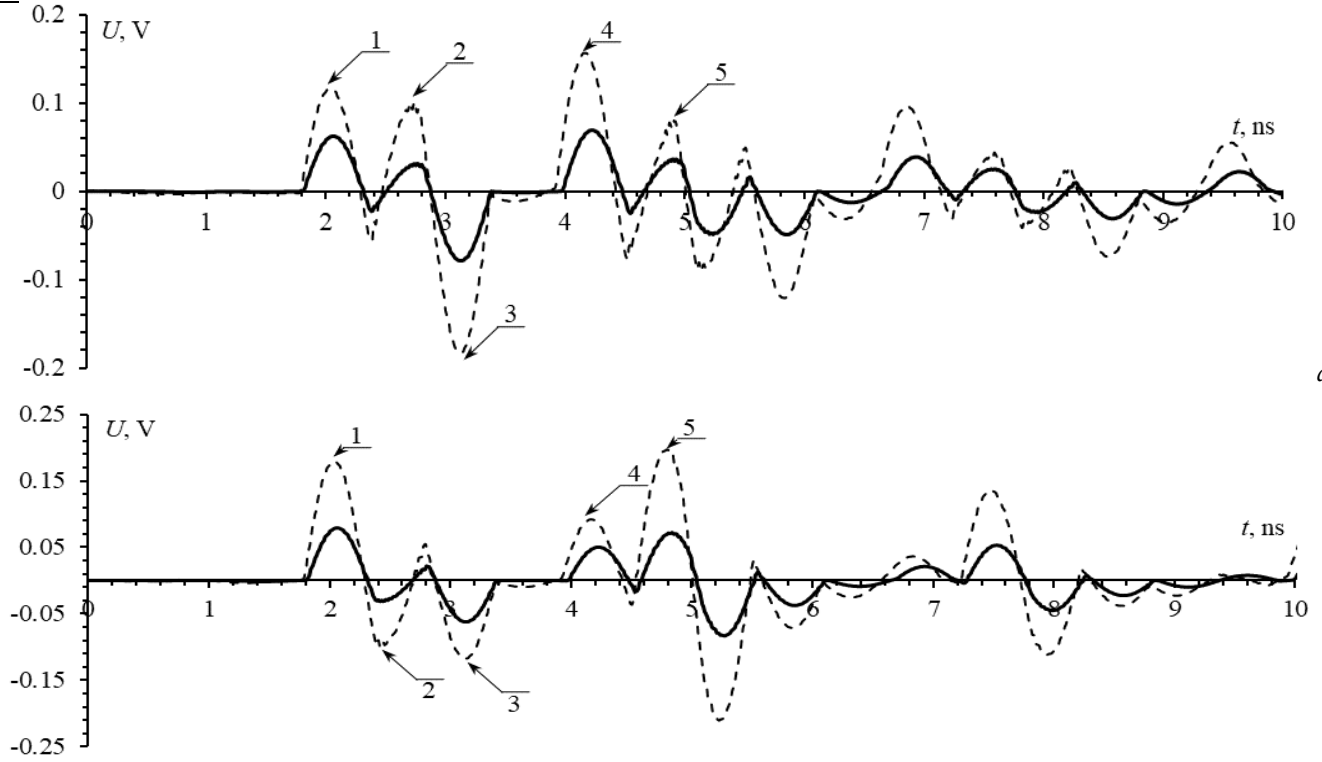


Fig. 6. Voltage waveforms at the MF output in common (—) and differential (---) modes, for conductors: 1 and 4 (a), 2 and 3 (b)

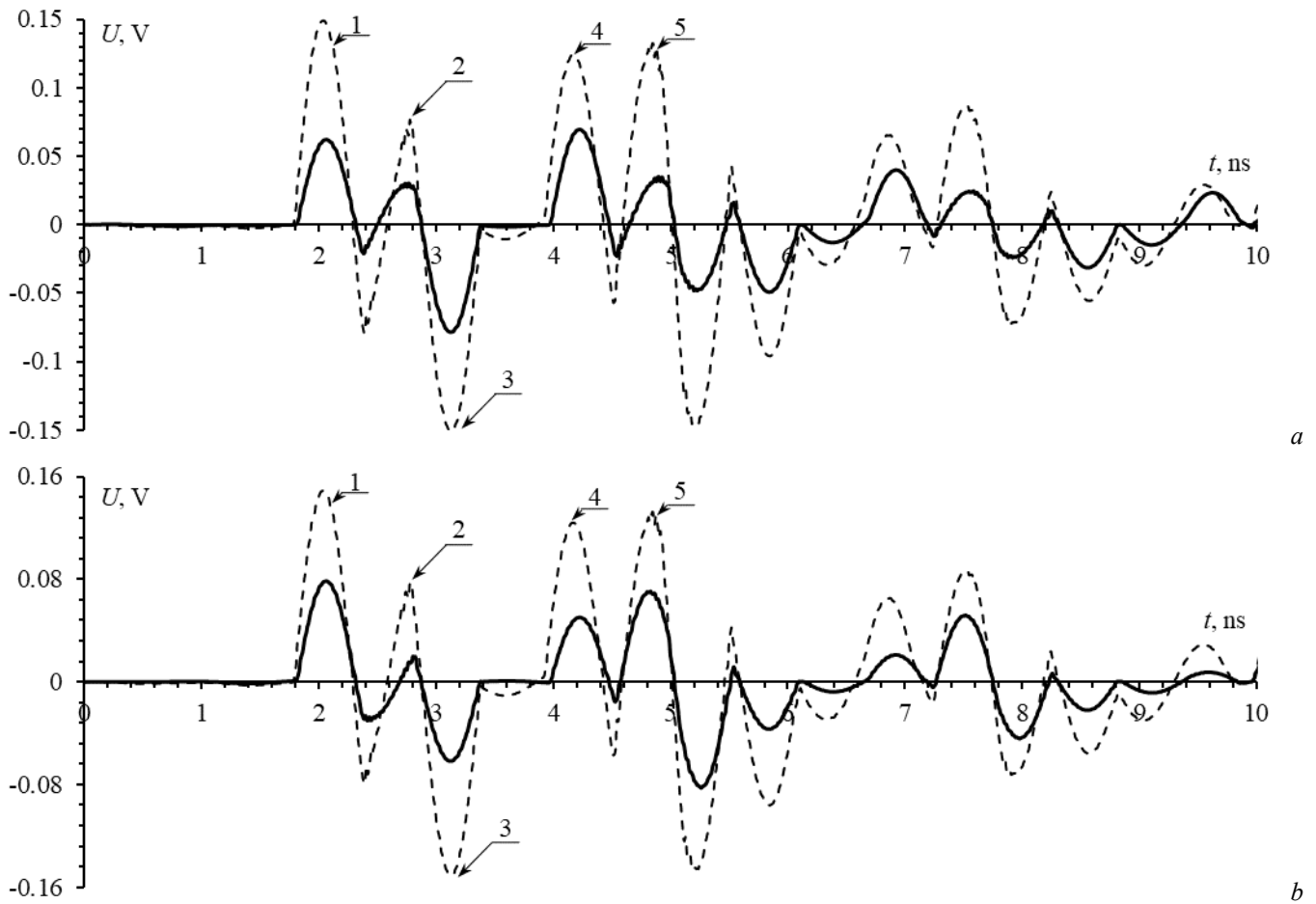


Fig. 7. Voltage waveforms at the MF output in common (—) and differential (---) modes, for conductors: 1 and 3 (a), 2 and 4 (b)

### III. CONCLUSION

Using a configuration with unequal characteristics can be useful to account for channel degradation due to component aging or wear. Using this configuration allows predicting the degradation trend of their characteristics in common and differential modes. Knowing the trends of component characteristics as they degrade, it is possible to switch to the required circuit at the right moment, thus compensating for the change in their characteristics. Configuration with equal characteristics can be used in cases where it is necessary to ensure the continuity of system operation without any change in its characteristics during the transition between active and passive circuits. The approach considered is acceptable in areas where it is acceptable to use switches at both the beginning and the end of a conductor with MR. Thus, it may be appropriate for dedicated and critical traces, allowing to achieve stable and reliable system operation in a wide range of operating conditions.

### REFERENCES

- [1] "IEEE approved draft standard for environmental and testing requirements for devices with communications functions used with electric power apparatus," in IEEE P1613/D3.2, May 2023, vol., no., pp.1-47, 28 Sept. 2023.
- [2] Y. J. Liu, T. P. Chang, H. W. Chen, T. K. Chang and P. H. Lan, "Power quality measurements of low-voltage distribution system with smart electric vehicle charging infrastructures," 2014 16th International Conference on Harmonics and Quality of Power (ICHQP), Bucharest, Romania, 2014, pp. 631-635.
- [3] N. Mora, F. Vega, G. Lugrin, F. Rachidi and M. Rubinstein, "Study and classification of potential IEMI sources," System Design and Assessment Notes, 2014, pp. 1-92.
- [4] D. V. Telpukhov and T. D. Zhukova, "New metric for evaluating the effectiveness of redundancy in fault-tolerant logic circuits," 2021 IEEE East-West Design & Test Symposium (EWDTS), Batumi, Georgia, 2021, pp. 1-6.
- [5] V. R. Sharafutdinov and T. R. Gazizov, "Analysis of reservation methods based on modal filtration," Systems of Control, Communication and Security, 2019, no. 3, pp. 117-144 (in Russ.).
- [6] A. Bukreev, A. Vinogradova and A. Vinogradov, "Seasonal redundancy of power supply to rural consumers," 2023 5th International Conference on Control Systems, Mathematical Modeling, Automation and Energy Efficiency (SUMMA), Lipetsk, Russian Federation, 2023, pp. 914-918.
- [7] E. Sisinni et al., "Investigating redundancy of LoRaWAN for emergency notifications in industrial plants," 2021 17th IEEE International Conference on Factory Communication Systems (WFCS), Linz, Austria, 2021, pp. 15-18.
- [8] M. Greco and C. Hernandez, "Heuristic function to solve the generalized covering tsp with artificial intelligence search," 2020 39th International Conference of the Chilean Computer Science Society (SCCC), Coquimbo, Chile, 2020, pp. 1-8.
- [9] IPC-2221 Generic Standard on Printed Board Design. Northbrook, Illinois: IPC, p. 124
- [10] A. M. Lakoza, V. P. Kosteletskii and A. M. Zabolotsky, "Estimating the Insertion attenuation under different methods of modal redundancy in

## 2024 International Conference on Industrial Engineering, Applications and Manufacturing (ICIEAM)

- differential and common modes,” 2023 International Ural Conference on Electrical Power Engineering (UralCon), Magnitogorsk, Russian Federation, 2023, pp. 408–412, doi: 10.1109/UralCon59258.2023.10291125.
- [11] Y. W. Hsu, S. J. Shen, C. A. Chen, S. H. Qiu and H. H. Chen, “Broadband measurement of dielectric constant on FR-4 PCB by using discontinuous microstrip Lines,” 2021 International Symposium on Antennas and Propagation (ISAP), Taipei, Taiwan, 2021, pp. 1–2.
- [12] IEC 61000–2–13. Electromagnetic compatibility (EMC). Part 2–13: environment. High-power electromagnetic (HPEM) environments. Radiated and conducted. Moscow, Standartinform Publ., 2013. Available at: <https://standards.globalspec.com/std/574272/IEC%2061000-2-13> (accessed 12.02.2024)
- [13] G. Jiandong, Z. Yue, L. Xiaoguang, S. Kaiyi, Z. Haoseng and M. Mingyu, “Design of common mode and differential mode separator for electromagnetic noise based on autotransformer,” 2021 IEEE International Joint EMC/SI/PI and EMC Europe Symposium, Raleigh, NC, USA, 2021, pp. 878–881.
- [14] V. P. Kosteletskii, E. B. Chernikova and A. M. Zabolotsky, “Development of a high current protection device against ultrashort pulse,” 2023 International Conference on Industrial Engineering, Applications and Manufacturing (ICIEAM), Sochi, Russian Federation, 2023, pp. 312–316, doi: 10.1109/ICIEAM57311.2023.10139254
- [15] A. M. Lakoza and V. P. Kosteletsky, “The Efficiency of Conductor Placement in Circuits with Single Modal Redundancy in Differential and Common Modes,” 2023 IEEE 24th International Conference of Young Professionals in Electron Devices and Materials (EDM), Novosibirsk, Russian Federation, 2023, pp. 1210–1214, doi: 10.1109/EDM58354.2023.10225177
- [16] S. P. Kuksenko, Preliminary results of TUSUR University project for design of spacecraft power distribution network: EMC simulation, *Journal of physics: conference series*, 2019, Vol. 560, Iss. 1. P. 012110. - DOI: 10.1088/1757-899X/560/1/012110
- [17] S. P. Kuksenko, A. M. Zabolotsky, A. O. Melkozerov and T. R. Gazizov, “New features of electromagnetic compatibility in TALGAT simulation software,” *Doklady TUSUR*, vol. 2, no. 36, 2015, pp. 45–50.